Local Charge Disproportion in a High-Performance Perovskite

Mirko Arnold,*,† Qiang Xu,‡ Frans D. Tichelaar,‡ and Armin Feldhoff†

Institute of Physical Chemistry and Electrochemistry, Leibniz Universität Hannover, Callinstrasse 3-3A, D-30167 Hannover, Germany, and National Centre for High Resolution Electron Microscopy, Technical University Delft, Lorentzweg 1, 2628 CJ Delft, The Netherlands

Received October 13, 2008. Revised Manuscript Received December 7, 2008

The temperature-dependent local charge disproportion in the $(Ba_{0.5}Sr_{0.5})(Co_{0.8}Fe_{0.2})O_{3-\delta}$ perovskite-type oxide (denoted as BSCF) was monitored by in situ electron energy-loss spectroscopy applying monochromized electrons in a transmission electron microscope. At elevated temperatures, oxygen is removed from the crystal lattice in these perovskite-type oxides that is due to a reduction of the transition metal sites. To determine the site-specific valence in the BSCF perovskite, we measured the cobalt and iron L-edges and the oxygen K-edge on increasing the temperature from 298 to 1223 K. It was found that the loss of oxygen at elevated temperatures is mainly due to a reduction of the cobalt site compared to the iron site. The understanding of the site specific redox behavior in this material is important in explaining its long-term instability at intermediate temperatures, which has not been elucidated priory this study.

Introduction

With the invention of mixed ionic and electronic conductive (MIEC) ceramics, a fast growing new branch in materials science has been established. Besides possessing a variety of fascinating properties, they are widely used as oxygen semipermeable membranes.[1] Because of their unique mixed conductivity properties, these materials are nowadays applied to two major processes. One application of MIECs is in solid-oxide fuel cells (SOFCs) where MIECs can be installed as cathode materials.[2] The second important application of MIECs is found in membrane reactors, where catalytic processes are combined with oxygen separation.[3,4]

The fundamental principle behind oxygen separation from gaseous mixtures via MIEC membranes is the ambipolar transport of oxygen ions and electrons through the MIEC crystal lattice. By applying a gradient in the oxygen chemical potential between two half-spaces separated by the MIEC membrane, oxygen ions move through the MIEC membrane from the higher to the lower chemical potential.[1,3−5] Permeation fluxes are significantly enhanced by the amount of mobile oxygen vacancies[1,5] in the crystal lattice because of the Nernst−Einstein equation, which gives a linear relationship between the ionic conductivity and the concentration of the oxygen vacancies. Removal of oxygen is accompanied by the reduction of the B-site transition metal (TM), which is therefore found in a variety of different valences.

It has already been proven by neutron diffraction and thermal gravimetry that oxygen stoichiometry ranges from ∼2.5 (at $T = 298$ K) down to ∼2.2 (at $T = 1173$ K) in $(Ba_{0.5}Sr_{0.5})(Co_{0.8}Fe_{0.2})O_{3-\delta}$ (denoted BSCF) without collapsing into a brownmillerite phase, thereby making BSCF an excellent oxygen conductor in the high temperature regime.[6,7] However, the element specific reduction is still unknown. In other words, it is not known to what extent cobalt or iron is reduced, but the local charge disproportion of MIECs at elevated temperatures is an important key in the understanding the phase stability and the electrical conductivity.[8,9] Švarcová et al. pointed out that the oxidation of the B-site cations leads to the phase instability of the BSCF at lower temperatures, because of the change in the effective ionic radii.[8]

To address the question of phase stability, the valence and spin state of the B-site cations must be determined, and such information cannot be provided from neutron or X-ray diffraction. The valence and spin state is strongly connected with the metal−oxygen distance and thus with the phase stability.[10] Particularly, if two different B-site cations are employed, a clear valence association is necessary in order to develop sophisticated explanations. For example, $Sr(Co_{0.8}Fe_{0.2})O_{3-\delta}$ (denoted as SCF) which is one end member within the system $(Ba_xSr_{1-x})(Co_{0.8}Fe_{0.2})O_{3-\delta}$, ex-

* Corresponding author. E-mail: Mirko.arnold@pci.uni-hannover.de. Phone: 0049-511-762-4896. Fax:0049-511-762-19121.
† Leibniz Universität Hannover.
‡ Technical University Delft.

(1) Bouwmeester, H. J. M.; Burggraaf, A. J. In *Fundamentals of Inorganic Membrane Science and Technology*; Burggraaf, A. J., Cot, L., Eds.; Elsevier: Amsterdam, 1996; pp 435−528.
(2) Shao, Z. P.; Haile, S. M. *Nature* **2004**, *431*, 170.
(3) Chen, C. S.; Feng, S. J.; Ran, S.; Zhu, D. C.; Liu, W.; Bouwmeester, H. J. M. *Angew. Chem.* **2003**, *115*, 5354−5356; *Angew. Chem. Int. Ed.* **2003**, *42*, 5196−5198.
(4) Caro, J.; Wang, H. H.; Tablet, C.; Kleinert, A.; Feldhoff, A.; Schiestel, T.; Kilgus, M.; Kölsch, P.; Werth, S. *Catal. Today* **2006**, *118*, 128–135.
(5) Zeng, P. Y.; Chen, Z. H.; Zhou, W.; Gu, H. X.; Shao, Z. P.; Liu, S. M. *J. Membr. Sci.* **2007**, *291*, 148–156.
(6) McIntosh, S.; Vente, J. F.; Haije, W. G.; Blank, D. H. A.; Bouwmeester, H. J. M. *Chem. Mater.* **2006**, *18*, 2187–2193.
(7) Vente, J. F.; McIntosh, S.; Haije, W. G.; Bouwmeester, H. J. M. *J. Solid State Electrochem.* **2006**, *10*, 581–588.
(8) Švarcová, S.; Wiik, K.; Tolchard, J.; Bouwmeester, H. J. M.; Grande, T. *Solid State Ionics* **2008**, *178*, 1787–1791.
(9) Goodenough, J. B. In *Structure and Bonding*; Mingos, D. M. P., Ed.; Springer: Berlin, 2000; Vol. 98, pp 1−15.
(10) Shannon, R. D. *Acta Crystallogr., Sect. A* **1976**, *A32*, 751–767.

10.1021/cm802779f CCC: $40.75
Published on Web 01/27/2009

hibits a phase transition from cubic perovskite to brownmillerite at elevated temperatures, and oxygen vacancies become immobile, resulting in a reduced oxygen conductivity.[11] Differences in the local charge distribution between BSCF and SCF might be useful to explain the difference in this behavior.

In this work, we present an in situ high-resolution electron energy-loss (HR-EELS) study in order to probe the local charge distribution and oxygen nonstoichiometry in BSCF. EELS is used to measure the energy-loss of electrons that interact with the sample and is a valuable tool to investigate the local environment of probe atoms. Sharp ionization edges occur if the core level electrons are excited to unoccupied electronic states by high-energy electrons from a transmission electron microscope. Information obtained by EELS is almost identical to X-ray absorption spectroscopy (denoted as XAS) and are therefore used equivalently in this study. By analyzing the electron energy-loss near-edge structure (ELNES), it is possible to obtain detailed structural and charge information of the investigated element.[12−14] Because the electronic structure of unoccupied states is influenced by the chemical environment, ELNES can provide the coordination, spin states, and valence of a particular element.[12−14] Another benefit of EELS is the high spatial resolution compared to other methods that are also used to probe the electronic environment in solids, such as XAS and X-ray photoelectron spectroscopy (XPS). This is an important issue with regard to local inhomogeneities that are inherent in these materials. Here we present HR-EELS data from a BSCF sample acquired by monochromized electrons operated in a transmission electron microscope. Monochromized electrons combine the advantages of high spatial resolution with high energy resolution (better than 0.15 eV), which enables the local charge distribution to be probed in very fine detail.[15] Additionally, transmission electron microscopes equipped with monochromators were specially designed for high energy stability, thus strongly reducing the shift of the peak positions.[15,16]

Experimental Section

In situ EELS. Thermal treatment and in situ EELS were performed on a FEI Tecnai-200FEG monochromator, equipped with a prespecimen monochromator and a high-resolution Gatan Imaging Filter (GIF) for EELS and single tilt heating holder (model 628, Gatan Inc., Pleasanton, CA). The specimen holder was water-cooled to allow operation at high temperatures (up to 1573 K) and to prevent specimen drift. All parts of the hot stage were made of tantalum. The furnace temperature was controlled using a miniature encapsulated 10 W heater. During heat treatment, the temperature was adjusted with a potentiometer controller by setting the heater current to the desired values. For HR-EELS acquiring, the high tension was set to 200 kV. The probe size was around 50−100 nm. All spectra were recorded in diffraction mode with entrance aperture 0.65 mm and camera length 200 mm. The energy resolution was measured in each experiment as the full width at half-maximum (fwhm) of the zero loss peak (ZLP), as acquired on the specimen. In order to maintain optimal energy resolution, a series of spectra, each acquired with short acquisition time (typically 15−20s for one spectra for the cobalt-L or the iron L-edge) were recorded. Data processing was conducted as following. First, all spectra were background subtracted using the power law model implemented in the Gatan Digital Micrograph software (version 1.70.16). Each spectrum was then adjusted by the ZLP and following, several spectra for each edge and temperature were aligned and summed to improve the signal-to-noise ratio. To determine the absolute peak position, we fitted the edges using several Gaussian functions. The weighted medium of the Gaussian functions was then taken as the absolute peak position of the edges. In the case of the oxygen K-edge, the area below the pre-edge peak (part A) as well the area below the first energy range (4 eV window) of part B (denoted as B_1 in Figure 4) were also determined by Gaussian fits in order to estimate the intensity ratio.

TEM Sample Preparation. BSCF samples were prepared by the commonly applied sol−gel synthetic route. Proper amounts of the metal nitrates were dissolved in water and ethylene-diaminetetraacetic acid (EDTA), citric acid and ammonia were added. The mixture was then heated to obtain dark-purple colored gel, which was then calcined for 5 h at $T = 1223$ K. Phase purity was determined by X-ray diffraction. The calcined powders were uniaxially cold pressed (at 140 kN) to get "green" bodies, which were then sintered at $T = 1423$ K for 10 h. The sintered membranes were polished down to a thickness of approximately 80 μm with polymer-embedded diamond lapping films (Allied High Tech, Multiprep). Polished samples were dimpled reaching a maximum thickness of 10 μm at the center of the membrane. Finally, the dimpled membranes were Ar^+-sputtered to achieve electron transparency (Gatan, model 691 PIPS, precision ion polishing system).

Results and Discussion

In order to investigate the electronic structure in BSCF, the cobalt-$L_{2,3}$, iron-$L_{2,3}$, and the oxygen K-edge were examined. The $L_{2,3}$-edges of cobalt and iron display an electronic transition from the transition metal's (TM) 2p core orbitals (split into $2p_{1/2}$ and $2p_{3/2}$ by spin−orbit coupling) to the partly unoccupied 3d orbitals, which are hybridized with oxygen 2p orbitals.[14] Figure 1 displays a simplified energy diagram in BSCF and qualitatively shows the important electronic transitions present in the discussed EELS experiment and reflects the fundamental idea of Goodenough. Basically, a valence band (VB) of mostly oxygen 2p character and an empty antibonding band of mostly the cation s and p character are formed due to a strong overlap of these orbitals.[9] The VB and the antibonding band are separated by a large band gap in which the hybridized TM 3d orbitals as well as the oxygen 2p fraction of this hybridization are located. Because of the excitation into the 3d orbitals, it is possible to obtain information about the chemical environment since the 3d orbitals mainly contribute to the bonding of the 3d TM. However, the $L_{2,3}$-edges of TMs exhibit complex patterns due to the strong overlap of the core wave function with valence wave functions (strong 3d−2p interactions) as well as the 3d−3d interactions. Therefore, a huge splitting of the electronic states and thus a complex spectrum

(11) McIntosh, S.; Vente, J. F.; Haije, W. G.; Blank, D. H. A.; Bouwmeester, H. J. M. *Solid State Ionics* **2006**, *177*, 833–842.
(12) Egerton, R. F.; Malac, A. *J. Electron Spectrosc. Relat. Phenom.* **2005**, *143*, 43–50.
(13) Egerton, R. F. *Electron Energy-Loss Spectroscopy in the Transmission Electron Microscope*; Plenum Press: New York, 1986.
(14) De Groot, F. M. F. *Coord. Chem. Rev.* **2005**, *249*, 31–63.
(15) Mitterbauer, C.; Kothleitner, G.; Grogger, W.; Zandbergen, H.; Freitag, B.; Tiemeijer, P.; Hofer, F. *Ultramicroscopy* **2003**, *96*, 469–480.
(16) Potapov, P. L.; Schryvers, D. *Ultramicroscopy* **2004**, *99*, 73–85.

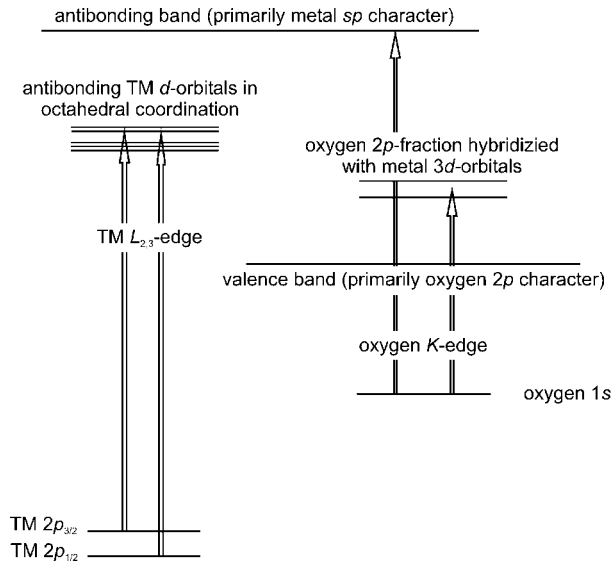

Figure 1. Qualitative energy diagram in BSCF. Electron transition of the TM $L_{2,3}$-edges and the oxygen K-edge are indicated by arrows.

were found.[12−15,17−19] The spectral features of the $L_{2,3}$-edges, and the absolute peak positions provide information about the chemical environment. This is the valence state of the TM, unless the local symmetry remain constant.[14,20] Because of an increase in the net formal charge of the TM, a shift in the $L_{2,3}$-edges toward higher energy was observed because the positively charged nucleus is less screened and higher energy is required to excite the core electrons to the outer electron orbitals.[21]

The local charge disproportion between oxygen and the TM is reflected in both the metal $L_{2,3}$-edge as well as in the oxygen K-edge because of the hybridization of the orbitals.[22] The oxygen K-edge, when hybridized with a lighter TM, is roughly separated into two parts, namely part A and part B.

The ground-state can be written as $\Phi_G = \alpha|d^n> + \beta|d^{n+1}\underline{L}>$ where $d^{n+1}\underline{L}$ describes the ligand hole configuration. According to Gloter et al., the intensity of peak A, which is proportional to β^2, is a measure for the covalency in the ground state. And, because of the fact that covalency increases with the formal valence for a given TM, the development of the oxygen prepeak (peak A) is a measure for the development of the oxidation state of the TM. [23,24]

Additional information can be obtained from the energy difference between parts A and B. A larger energy difference between parts A and B with increasing iron valence has already been reported.[24,25] Colliex et al. found an energy difference of 9.0 eV (Fe^{2+}) and 10.9 eV (Fe^{3+}), respectively.[24] Therefore, also the energy difference between the two parts of the oxygen *K*-edge can provide additional evidence for a reduction of the TM.

Following these arguments, a shift of the absolute peak positions of the $L_{2,3}$-edges for cobalt and iron as well as the change of the ratio of relative intensities and the energy difference within the oxygen *K*-edge were analyzed. Because reduction of the B-site TM was noticed at elevated temperatures and the fact that BSCF membranes are commonly operated between $T = 973$ K and $T = 1223$ K, the HR-EELS experiments were performed using a heatable sample holder at temperatures up to $T = 1223$ K.

It should be noted that other methods, which can be used to determine the formal valence of TM in oxides or other compounds from EELS data, are not suitable in the present study. One method is based on the idea that any sample under investigation is a mixture of TMs with different distinct valences,[26] and thus the acquired spectra are simply the overlaid spectra from known compounds. The formal intermediate valence is therefore calculated by the fraction of each species in the sample. Methods to deconvolute these spectra are discussed in detail by Calvert et al.[27] This method is not applicable to the present study because the valence of the TM in BSCF is not an average of isolated distinct valences but rather each TM ion displays an intermediate valence. Therefore the acquired spectra for the TM in BSCF are not simply overlaid spectra of known standards.

Another method requires determining the TM L_3/L_2 intensity ratio,[28,29] which is also sensitive to the TM valence. The L_3/L_2 intensity ratio method is not applicable to the current study since the cobalt $L_{2,3}$-edges overlap with the barium $M_{4,5}$-edge, making it very difficult to accurately determine the whole peak area and therefore to determine the intensity ratio.

Figure 2 presents the temperature development of the cobalt L_3-edge compared with the well-known materials, Co_3O_4 and CoO (Figure 2a) as well as a plot of its absolute energy position and its symmetry (Figure 2b). The spectra can be evaluated with regard to the peak shape and the absolute peak position. The peak shape will be discussed only qualitatively because many components contribute to the spectral shape, and a quantitative discussion might be rather speculative, particularly if the temperature is raised. The absolute peak position can be more reliably addressed because of the low energy drift of the electron microscope used in the experiment.[15] Additionally, the shift of the cobalt L_3-edge can be related to the position of the barium M_5-edge, because the energy difference between these two lines is not larger than 5 eV. Thus, it is possible to use the inert

(17) Zaanen, J.; Sawatzky, G. A.; Fink, J.; Speier, W.; Fuggle, J. C. *Phys. Rev. B* **1985**, *32*, 4905–4913.
(18) Abbate, M.; Fuggle, J. C.; Fujimori, A.; Tjeng, L. H.; Chen, C. H.; Potze, R.; Sawatzky, G. A.; Eisaki, H.; Uchida, S. *Phys. Rev. B* **1993**, *47*, 16124–16130.
(19) Hu, Z.; Wu, H.; Haverkort, M. W.; Hsieh, H. H.; Lin, H. J.; Lorenz, T.; Baier, J.; Reichl, A.; Bonn, I.; Felser, C.; Tanaka, A.; Chen, C. T.; Tjeng, L. H. *Phys. Rev. Lett.* **2004**, *92*, 207402-1–207402-4.
(20) Paterson, J. H.; Krivanek, O. L. *Ultramicroscopy* **1990**, *32*, 319–325.
(21) Yoon, W. S.; Kim, K. B.; Kim, M. G.; Lee, M. K.; Shin, H. J.; Lee, J. M.; Lee, J. S. *J. Phys. Chem. B* **2002**, *106*, 2526–2532.
(22) De Groot, F. M. F.; Grioni, M.; Fuggle, J. C.; Ghijsen, J.; Sawatzky, G. A.; Petersen, H. *Phys. Rev. B* **1989**, *40*, 5715–5723.
(23) Gloter, A.; Ingrin, J.; Bouchet, D.; Colliex, C. *Phys. Rev. B* **2000**, *61*, 2587–2594.
(24) Colliex, C.; Manoubi, T.; Ortiz, C. *Phys. Rev. B* **1991**, *44*, 11402–11411.
(25) Chen, J. G.; Frühberger, B.; Colaianni, M. L. *J. Vac. Sci. Technol., A* **1995**, *14*, 1668–1673.
(26) Garvie, L. A. J.; Buseck, P. R. *Nature* **1998**, *396*, 667–670.
(27) Calvert, C. C.; Brown, A.; Brydson, R. *J. Electron Spectrosc. Relat. Phenom.* **2005**, *143*, 173–187.
(28) Pearson, D. H.; Ahn, C. C.; Fultz, B. *Phys. Rev. B* **1993**, *47*, 8471–8478.
(29) Wang, Z. L.; Yin, J. S.; Mo, W. D.; Zhang, Z. J. *J. Phys. Chem. B* **1977**, *101*, 6793–6798.

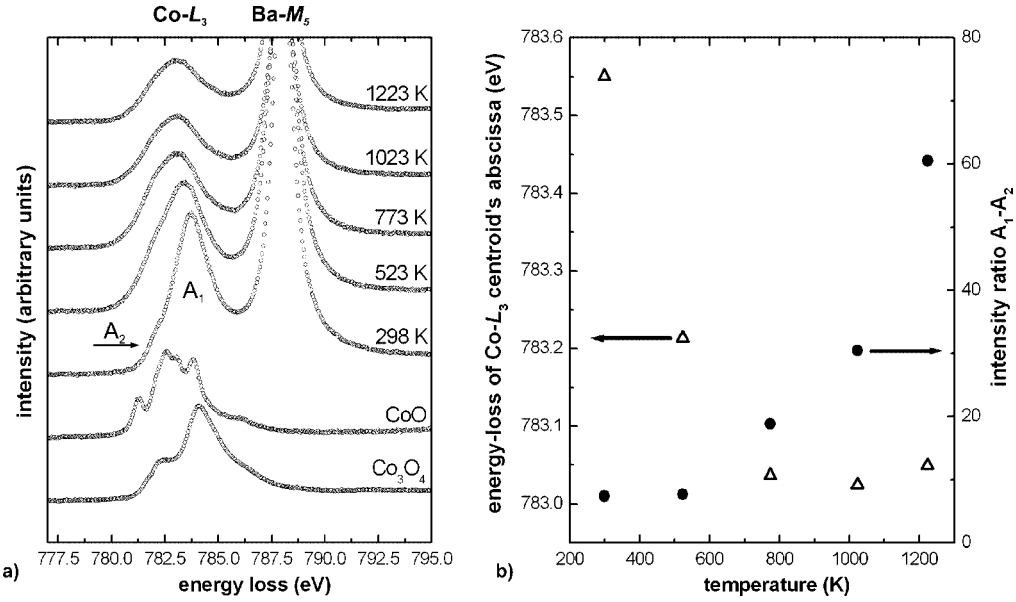

Figure 2. (a) Temperature-dependent evaluation of the cobalt-L_3 and the barium M_5-edge in BSCF compared to the cobalt L_3-edge in Co_3O_4 and CoO. The error of the absolute energy position was determined to be ±0.1 eV. (b) Plot of the cobalt L_3 centroid's abscissa and relative intensity of the low-energy shoulder (as indicated by the arrow) compared to the main peak versus temperature.

barium M_5-edge as an internal standard since the electronic structure of barium in BSCF does not change with increasing temperature.

At room temperature, the peak shape was consistent with a Co^{3+} in a high spin configuration simulated and measured by Hu et al.[19] (pyramidal coordination) and Lozano-Gorrin et al.[30] (octahedral coordination). Comparing the absolute energy value of the cobalt in BSCF with the absolute energy values of CoO (Co^{2+}) and Co_3O_4 ($Co^{2.67+}$), we concluded that the cobalt in BSCF has a formal charge of +2.60 with a predominately high spin configuration in BSCF. We used the centroid's absolute energy position of the Co L_3-edge in CoO and Co_3O_4 (Co^{2+}: 782.80 eV, $Co^{2.67+}$: 783.63 eV) and, by assuming a linear function between these two valence states, we identified the cobalt valence in BSCF. It is clear from Figure 2 that increasing the temperature caused a shift of the absolute peak position of the cobalt L_3-edge as well as a vanishing of the low energy shoulder (higher symmetry of the peak). Figure 2b displays the absolute peak position and the intensity of the low energy shoulder (A_2) compared with the main peak (A_1). We can rationalize the absolute energy shift as resulting from a decrease in the net formal valence of the cobalt (as is explained above). The cobalt valence decreased to +2.3 at $T = 523$ K and reached the minimum valence of +2.2 at $T = 773$ K (We emphasize that the absolute valence for both cobalt and iron are afflicted with a certain error as indicated below the Figures 2 and 3). Further increases in temperature did not change the valence of the cobalt, but symmetry and the broadening of the L_3-edge resulted in a pure Gaussian shape of the edge, which meant that no low energy shoulder could be observed at high temperatures. Several effects contributed to the pronounced symmetry of the L_3-edge and it was difficult to distinguish between these effects.

For example, excitation of lattice vibration (phonon broadening) or reduction of symmetry because of mobile oxygen vacancies may lead to the vanishing of the low energy shoulder.

The second B-site TM in BSCF is iron, and the temperature dependence of its L_3-edge is plotted in Figure 3 along with two standards, α-Fe_2O_3 (octahedral Fe^{3+}) and $FeTiO_3$ (octahedral Fe^{2+}). At room temperature, we found that the iron was predominately in a 3+ high spin valence state, which was in good agreement with the findings of Paterson et al.,[2420] who compared the $L_{3,2}$-edge of α-Fe_2O_3 and γ-Fe_2O_3 and reported not only a remarkable difference in the absolute energy position but more importantly, a different splitting of the edges, which is independent from energy drifts of the instrument. By comparing the energy position as well as the splitting of the iron L_3-edge in BSCF with α-Fe_2O_3 and the results of Paterson et al., we come to the conclusion that the iron is indeed in the +3 valence state, though it differs from the measured α-Fe_2O_3. Increases in temperature led to a decrease in the iron's valence of +2.7 at $T = 523$ K. A valence state of +2.8 was reached after further temperature increases. As described for the case of cobalt, a linear fit between Fe^{3+} and Fe^{2+} was applied in order to determine the valence of iron at elevated temperatures.

Figure 4 shows a plot of the oxygen K-edge with increasing temperature. We found a significant increase of the intensity ratio, B/A, as well as a decrease in the energy difference between the B and A peaks. "Part A" and "Part B" were fitted using several Gaussian functions from which we determined the absolute peak positions and areas. For both parameters, drastic changes occurred between $T = 298$ and 773 K. Changes in the peak areas can be clearly attributed to the loss of oxygen, which causes a reduction of the cobalt and the iron, resulting in a formal valence of the B-site of +2.3. Besides changes in intensity, a decrease

(30) Lozano-Gorrin, A. D.; Greedan, J. E.; Nunez, P.; Gonzalez-Silgo, C.; Botton, G. A.; Radtke, G. *J. Solid State Chem.* **2007**, *180*, 1209–1217.

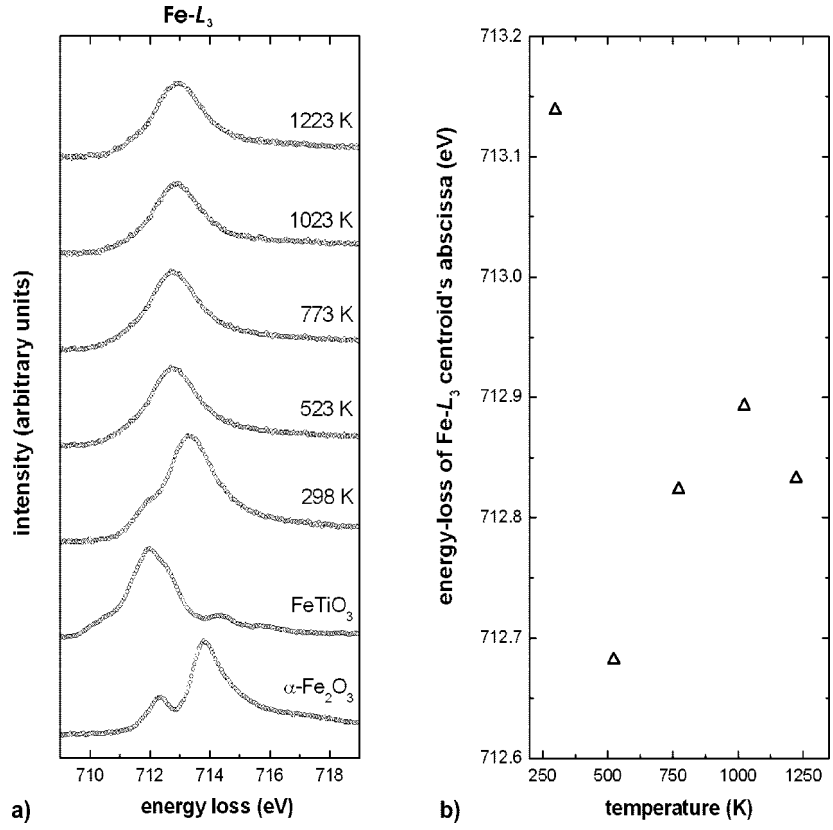

Figure 3. (a) Temperature-dependent evaluation of the iron L_3-edge in BSCF compared to the iron L_3-edge in α-Fe_2O_3 and $FeTiO_3$. The error of the absolute energy position was ± 0.1 eV. (b) Plot of the iron L_3 centroid's abscissa versus temperature.

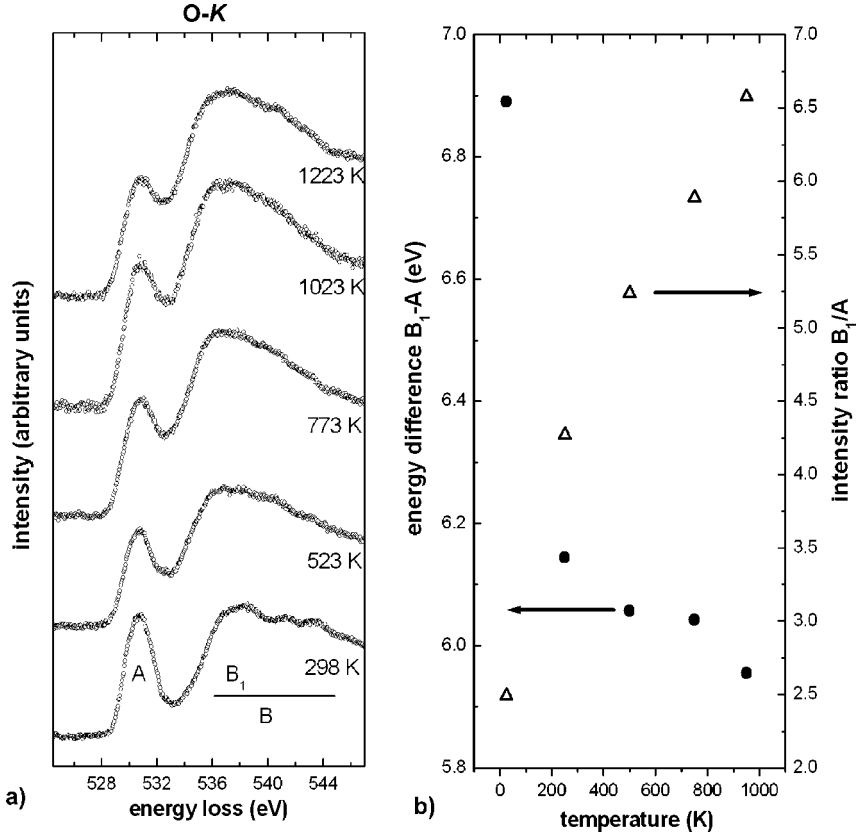

Figure 4. (a) Temperature-dependent evaluation of the oxygen K-edge in BSCF. (b) Plot of the energy difference and intensity ratio of feature A and B in the oxygen K-edge. Spectra were aligned with respect to the peak "A".

in the energy difference can rationalized, which is in good agreement with findings from Colliex et al.,[24] who found a smaller separation of peak A and B with decreasing valence of iron in investigated oxides. Further increases of temper-

Table 1. Summary of the Temperature-Dependent Evaluation of the B-Site Valence and Difference and Intensity Ratio of Feature A and B in the Oxygen K-Edge

	valence of B-site cation			oxygen site	
temperature (K)	cobalt	iron	sum	peak ratio B_1/A	peak difference $B_1 - A$ (eV)
298	2.6	3.0	2.7	2.49	6.89
523	2.3	2.7	2.4	4.26	6.14
773	2.2	2.8	2.3	5.24	6.06
1023	2.2	2.8	2.3	5.89	6.04
1223	2.2	2.8	2.3	6.57	5.96

ature (>773 K) left the summed valence of the B-site constant, and both the intensity ratio as well as the energy difference changed little within the oxygen K-edge (Figure 4b). These minor changes might be either due to a pronounced charge transfer toward the oxygen site at elevated temperatures or the lower sensitivity of the TM $L_{2,3}$-edge with regard to the reduction.

A summary of the key findings can be found in Table 1. The overall B-site valence decreased from +2.7 at $T = 298$ K to +2.3 between $T = 773$ and 1223 K, and cobalt was more strongly reduced relative to iron. Reduction on the B-site TM associated by the absolute peak position was in excellent agreement with findings at the oxygen K-edge. The intensity ratio of the peaks B/A as well as the energy difference between peaks B and A exhibited similar changes in the same temperature regime.

Conclusions

We have presented unambiguous evidence that oxygen removal in the mixed conductor BSCF is due to a reduction of the B-site TM, namely cobalt and iron, with the cobalt being more strongly reduced. Though the conditions in a TEM are not comparable to those in ambient air, the experiment provides the information that mainly cobalt is reduced in BSCF when increasing the temperature. Because $Co^{+2.2}$ is stable at high temperatures, BSCF's stability only at high temperatures is plausible. At lower temperatures, BSCF (and hence cobalt) is oxidized in air atmospheres and it is proposed that this yields the formation of hexagonal perovskites containing Co^{3+} in the low spin state.[8,31] Thus, the information reflecting the redox behavior of perovskites under ambient atmospheres, derived from neutron diffraction[6] as well as thermal gravimetric measurements[7] together with the element specific charge distribution obtained from the here presented in situ HR-EELS, provide the explanation of BSCF's stability at high temperatures only.

Note Added in Proof. Recent XANES investigations on $(Ba_{1-x}Sr_x)(Co_{1-y}Fe_y)O_{3-\delta}$ compounds quenched from different temperatures give a further hint to a spin state transition of trivalent cobalt.[32]

Acknowledgment. The authors greatly acknowledge financial support from the DFG (Grant FE 928/1−2), financial support from the European Union under the Framework 6 program under a contract for an Integrated Infrastructure Initiative. Reference 026019 ESTEEM. M.A. and A.F. appreciate fruitful discussions with Professor Jürgen Caro.

CM802779F

(31) Arnold, M.; Gesing, Th. M.; Martynczuk, J.; Feldhoff, A. *Chem. Mater.* **2008**, *20*, 5851–5858.
(32) Harvey, A. S.; Yang, Z.; Infortuna, A.; Beckel, D.; Purton, J. A.; Gauckler, L. J. *J. Phys.: Condens. Matter* **2009**, *21*, 015801–015810.